Acta Crystallographica Section D
Biological Crystallography
ISSN 0907-4449

Structure of D-ribulose 5-phosphate 3-epimerase from *Synechocystis* to 1.6 Å resolution

Eric L. Wise,[a]‡ Julie Akana,[b]‡ John A. Gerlt[b] and Ivan Rayment[a]*

[a]Deparment of Biochemistry, University of Wisconsin, Madison, WI 53706, USA, and [b]Departments of Biochemistry and Chemistry, University of Illinois, Urbana, IL 61801, USA

‡ These authors contributed equally to this work.

Correspondence e-mail: ivan_rayment@biochem.wisc.edu

Received 10 May 2004
Accepted 29 June 2004

PDB Reference: D-ribulose 5-phosphate 3-epimerase, 1tqj, r1tqjsf.

The crystal structure of D-ribulose 5-phosphate 3-epimerase (RPE) from the cyanobacterium *Synechocystis* was determined by X-ray crystallography to 1.6 Å resolution. The enzyme, which catalyzes the epimerization of D-ribulose 5-phosphate and D-xylulose 5-phosphate, assembles as a hexamer of $(\beta/\alpha)_8$-barrels in the crystallographic asymmetric unit. The active site is highly similar to those of two previously reported RPEs and provides further evidence for essential catalytic roles for several active-site residues.

1. Introduction

D-Ribulose 5-phosphate 3-epimerase (RPE) catalyzes the interconversion of D-ribulose 5-phosphate and D-xylulose 5-phosphate through an inversion of the stereochemical configuration at the 3′ carbon of either substrate (Fig. 1). Cytosolic RPEs in plants, yeast and animals have been shown to be involved in the oxidative pentose phosphate pathway that is critical for the generation of NADPH (Kopriva *et al.*, 2000). In addition, RPE is also found in the chloroplasts in plants, where it is involved in the reductive pentose phosphate pathway (Calvin cycle; Eicks *et al.*, 2002; Jelakovic *et al.*, 2003).

The X-ray crystal structures of spinach chloroplast RPE and cytosolic rice RPE have recently been reported and demonstrated that the enzyme adopts a $(\beta/\alpha)_8$-barrel fold and assembles as multimers (Jelakovic *et al.*, 2003; Kopp *et al.*, 1999). In the case of cytosolic rice RPE the enzyme forms a homodimer, while spinach chloroplast RPE forms a homohexamer. Although they share only around 40% sequence identity, the active sites of both RPEs are highly similar and contain several strictly conserved amino-acid residues, including a pair of aspartate residues and a pair of histidine residues. On the basis of the existing crystal structures, it has been proposed that the two strictly conserved aspartate residues act as catalytic acid/bases to alternately protonate and deprotonate C3 of either D-ribulose 5-phosphate or D-xylulose 5-phosphate. The observation that the two aspartate and two histidine residues can serve as ligands for a zinc ion in the cytosolic rice RPE structure led to the proposal that these four residues serve as ligands for a zinc ion that functions to stabilize a 2,3-enediolate reaction intermediate (Jelakovic *et al.*, 2003; Wise & Rayment, 2004). Alternatively, it was proposed that the two histidines stabilize the negative charge on either aspartate *via* a water molecule bound in place of the zinc ion; the S atoms on three conserved methionine residues would stabilize the reaction intermediate (Kopp *et al.*, 1999). Because the exact mechanism of the RPE-catalyzed reaction is unknown, the functions of the conserved active-site residues remain unclear. Here, we report the crystal structure of RPE from the cyanobacterium *Synechocystis* (seRPE) to 1.6 Å resolution. The enzyme shares a highly similar active site with the other two RPEs for which structure crystal structures are available, which further underscores the importance of conserved active-site residues in the catalytic mechanism.

2. Materials and methods

2.1. Cloning, protein expression and purification

The gene encoding RPE was cloned from *Synechocystis* genomic DNA using Platinum *Pfx* DNA polymerase (Life Technologies). The

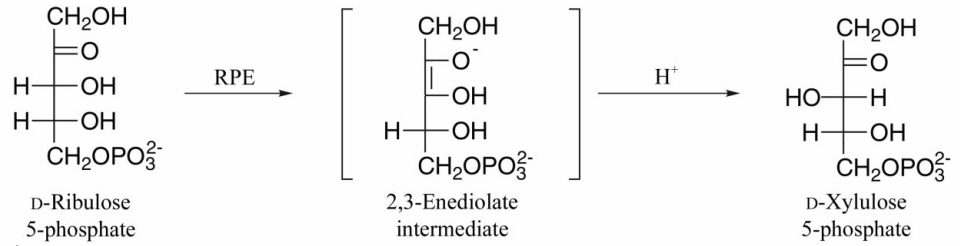

Figure 1
The reaction catalyzed by RPE.

genomic DNA was a gift from Dr Kancke at the Kazusa DNA Research Institute in Japan. The gene was amplified using the polymerase chain reaction (100 µl) containing 167 ng genomic DNA, 10 µl 10X *Pfx* amplification buffer, 1 m*M* $MgSO_4$, 0.4 m*M* of each dNTP, 40 pmol of each primer (forward primer 5′-CTTAGAGACCCTTCATATGTCCAAAAATATCGTCG-3′ and reverse primer 5′-CCATGGGCCTCGAGTTACACCGTTGCCAGTTG-3′) and 5 U Platinum *Pfx* DNA polymerase. A PTC-200 Gradient Thermal Cycler (MJ Research) was used with the following parameters: 367 K for 2 min followed by 40 cycles of 318 K for 1 min, a gradient temperature range of 318–338 K for 1 min 15 s, 345 K for 2 min 15 s and a final extension at 345 K for 10 min. The amplified gene was restriction-digested with *Nde*I and *Xho*I (New England BioLabs) and inserted into the pET15b (Novagen) plasmid. The pET15b vector added a six-His tag to the N-terminus of the recombinant protein. The protein was expressed in *Escherichia coli* BL21 (DE3) cells (Novagen). The transformed cells were grown at 298 K in LB broth and 100 µg ml^{-1} ampicillin for 24 h and harvested by centrifugation. The cells were resuspended in 5 m*M* imidazole, 0.5 *M* NaCl, 20 m*M* Tris–HCl pH 7.9, 5 m*M* $MgCl_2$ and lysed by sonication. The lysate was applied to a chelating Sepharose Fast Flow column (Pharmacia Biotech) charged with Ni^{2+}. The column was washed with 5% elution buffer (1 *M* imidazole, 0.5 *M* NaCl, 20 m*M* Tris–HCl pH 7.9, 5 m*M* $MgCl_2$)/95% wash buffer (60 m*M* imidazole, 0.5 *M* NaCl, 20 m*M* Tri–HCl pH 7.9, 5 m*M* $MgCl_2$) and the protein was eluted with 50% wash buffer/50% strip buffer (100 m*M* EDTA, 0.5 *M* NaCl, 20 m*M* Tris–HCl pH 7.9, 5 m*M* $MgCl_2$). The N-terminal His tag was removed by thrombin cleavage (Pharmacia Biotech) according to the manufacturer's instructions and the protein was dialyzed into storage buffer (50 m*M* Tris–HCl pH 7.9, 100 m*M* NaCl, 5 m*M* $MgCl_2$).

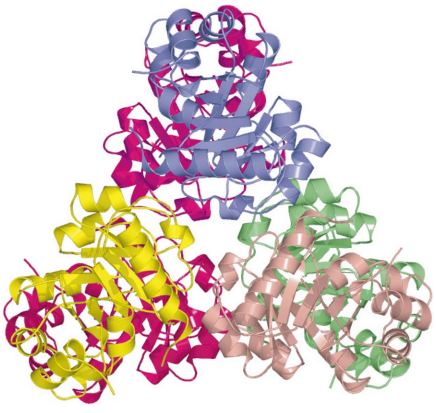

Figure 2
The seRPE crystallographic asymmetric unit. Six identical copies of seRPE are found in the asymmetric unit. The view is looking straight down a threefold non-crystallographic symmetry axis. Three twofold non-crystallographic symmetry axes lie perpendicular to the threefold axis. This figure was created with *PyMol* (DeLano, 2002).

2.2. Crystallization and data collection

Crystals of RPE were grown using the microbatch technique from 22% methyl ether PEG 2000, 200 m*M* $MgCl_2$, 100 m*M* MES pH 6.0 (Rayment, 2002). The crystals belonged to space group $P2_1$, with unit-cell parameters a = 82.6, b = 87.8, c = 97.8 Å, $\beta = 114.6^\circ$. The crystals were frozen prior to data collection by transferring them into a solution of 25% methyl ether PEG 2000, 200 m*M* $MgCl_2$, 100 m*M* MES pH 6.0, 20% PEG 400 and were flash-frozen in liquid nitrogen. Diffraction data were collected to 1.6 Å resolution using synchrotron radiation at beamline 14BM at the Advanced Photon Source. The data were integrated and scaled with the programs *DENZO* and *SCALEPACK* (Otwinowski & Minor, 1997).

2.3. Structure determination

An initial molecular-replacement solution was obtained using the structure of the potato chloroplast RPE structure (PDB code 1rpx) as a search model in the program *COMO* (Jogl *et al.*, 2001). The model was improved through automatic model building and refinement using the programs *ARP/wARP* and *REFMAC* and manual fitting using the program *TURBO-FRODO* (Collaborative Computational Project, Number 4, 1994; Murshudov *et al.*, 1997; Roussel & Cambillau, 1991; Terwilliger & Berendzen, 1999). Analysis with the program *PROCHECK* indicates that 93.2% of φ–ψ pairs for non-glycine residues fall in the most favorable region of a Ramachandran plot and the remaining 6.8% of residues fall in the additionally allowed regions (Laskowski *et al.*, 1993). Data-collection statistics and final refinement statistics are given in Table 1.

3. Results and discussion

3.1. Structure of seRPE

The seRPE crystallographic asymmetric unit contains six identical molecules of seRPE that assemble in a hexameric structure (Fig. 2). Each subunit adopts a $(\beta/\alpha)_8$-barrel fold comprised of a ring of eight β-strands surrounded by eight α-helices. All six subunits are essentially identical and the electron density for each subunit is clear for the entire length of the molecule, with the exception of the first two amino-acid residues, a region extending from Gly146 to Gln150 and the last seven amino-acid residues in the polypeptide chain. The disordered residues that extend from Gly146 to Gln150 are found in a loop region that has been associated with substrate binding. The structures of the potato chloroplast and cytosolic rice RPEs were both solved with a bound sulfate ion in the active site that was suggested to bind in the binding site for the phosphate group of the phosphorylated substrate. That the structure of seRPE is a 'true' apo structure without any analogous ion in the active site may explain why the region 146–150 is disordered in the structure.

Table 1
Data-collection and refinement statistics.

Space group	$P2_1$
Unit-cell parameters (Å, °)	a = 82.6, b = 87.8, c = 97.8, β = 114.6
Wavelength (Å)	0.900
Resolution range	50–1.60 (1.66–1.60)
Total reflections	1742997
Unique reflections	166356
R_{merge}† (%)	0.052 (0.336)
Completeness (%)	94.3 (91.9)
Average $I/\sigma(I)$	28.2 (4.1)
R_{work}‡ (%)	17.1
R_{free}‡ (%)	21.9
Average B factor (Å^2)	21.6
R.m.s.d. deviations	
Bond lengths (Å)	0.017
Bond angles (°)	1.63

† $R_{merge} = \sum|I_{hkl} - I|/\sum I_{hkl}$. ‡ R factor = $\sum|F_o - F_c|/\sum|F_o|$.

3.2. Comparison with other RPE structures

The overall arrangement of the individual monomers in the seRPE hexamer is highly similar to that observed in the potato chloroplast RPE structure. Each of the monomers in the asymmetric unit is related to the others by a threefold non-crystallographic axis and several twofold non-crystallographic axes that run perpendicular to the threefold NCS axis so that the overall complex has D_3 symmetry. The potato chloroplast RPE hexamer shares an identical symmetry arrangement to form a hexamer, although in the potato chloroplast structure the twofold symmetry axes that are perpendicular to that threefold axis lie along crystallographic twofold axes. The buried surface area between two monomers in the dimer is approximately 1050 Å^2, while the buried surface area between adjacent monomers related by the threefold axis is only 750 Å^2. The primary polypeptide

sequences for the potato chloroplast RPE and seRPE share approximately 60% sequence identity and when the structures of the monomers are aligned with the program *ALIGN*, the r.m.s.d. for paired C^{α} residues is approximately 0.5 Å^2 for 212 C^{α} atoms (Cohen, 1997). The overall r.m.s.d. for the seRPE hexamer and the potato chloroplast hexamer is 0.8 Å^2 for 1054 paired C^{α} atoms.

The seRPE structure also shares significant similarity with the structure of cytosolic rice RPE. Although cytosolic rice RPE only forms as a dimer rather than a hexamer, the arrangement of each of the three dimers formed by the twofold NCS axis in the seRPE and potato chloroplast structures are identical to the cytosolic rice RPE dimer (Fig. 3*a*). The sequences of each RPE share approximately 45% sequence identity and when the structures of the monomers are aligned the r.m.s.d. for paired C^{α} residues is approximately 1.0 Å^2 for 202 C^{α} atoms. The overall r.m.s.d. for the entire dimer is 1.3 Å^2 for 407 C^{α} atoms. In all three structures, the antiparallel arrangement of the individual subunits forming a dimer is perfectly conserved. The dimer interfaces in all three enzymes are highly conserved and are formed from conserved residues, while the residues involved in trimer association in seRPE and potato chloroplast RPE are not highly conserved in cytosolic rice RPE (Kopp *et al.*, 1999). Studies with human erythrocyte RPE suggested cooperative substrate binding with a Hill coefficient of 2, which might explain the importance of the conserved dimeric structure in all three RPEs (Karmali *et al.*, 1983).

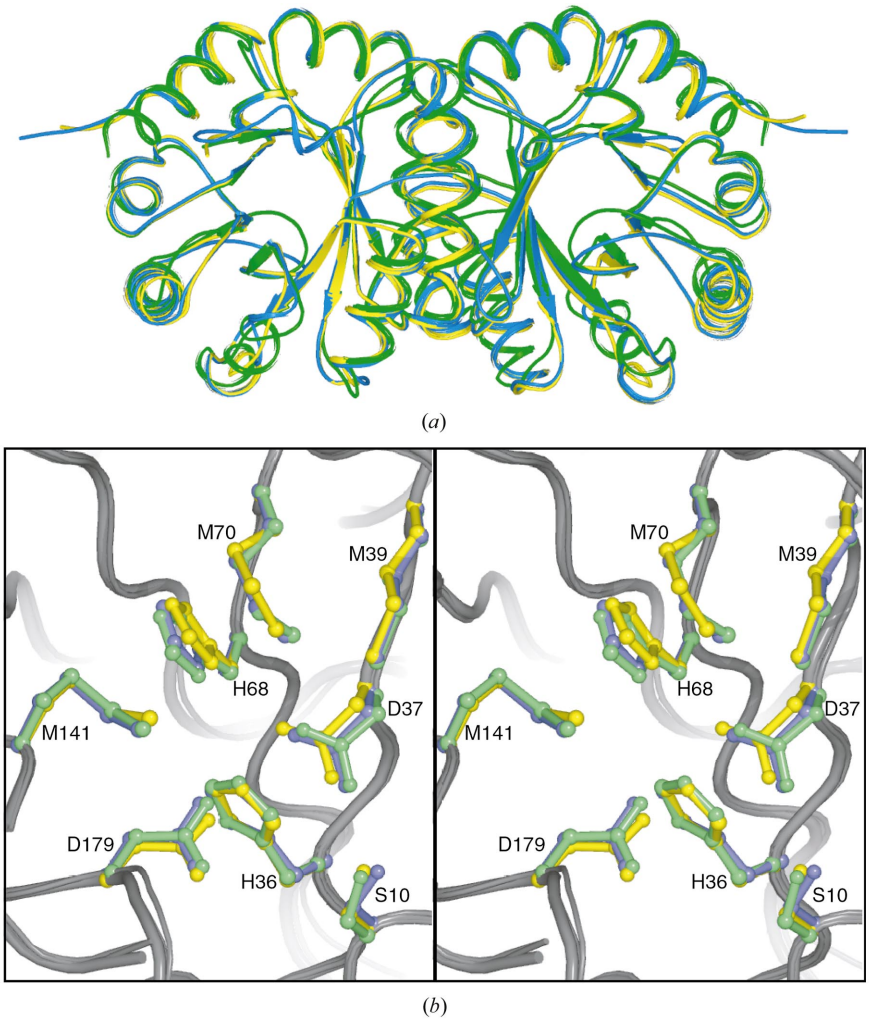

Figure 3
(*a*) Alignment of the RPE dimers from seRPE (yellow), potato chloroplast (blue) and cytosolic rice (green). In the case of seRPE and potato chloroplast RPE, the dimers themselves assemble into larger hexameric structures. (*b*) Stereo overlay of the active site of seRPE (yellow) and the active sites of the potato chloroplast RPE (blue) and the cytosolic rice RPE (green). The positions of two strictly conserved aspartate residues, Asp37 and Asp179, and two strictly conserved histidine residues, His36 and His68, are perfectly conserved in all three enzymes. In addition, three highly conserved methionines, Met39, Met70 and Met141, along with a highly conserved serine, Ser10, are also found in essentially identical positions in the active site. The figure was created with *PyMol* (DeLano, 2002).

3.3. RPE active site

The location of the active site and the overall positions of most residues in the active site of seRPE are nearly identical to those in the two other RPE structures. An overlay of the active sites of all three RPE structures shows that the positions and conformations of several catalytic residues are highly conserved in all three structures (Fig. 3). The positions of two strictly conserved aspartate residues, Asp37 and Asp179, and two strictly conserved histidine residues, His36 and His68, are almost perfectly conserved across all three RPE structures. These residues have been suggested to either function as ligands for a catalytic metal ion or to take part directly in acid/base catalysis (Chen *et al.*, 1999; Jelakovic *et al.*, 2003; Kopp *et al.*, 1999). While there is no direct biochemical evidence for the role of a metal ion in the RPE reaction, cytosolic rice RPE crystals soaked in the presence of zinc were shown to bind zinc in the active site using the histidine and aspartate pairs as ligands. Likewise, when crystals of seRPE were grown in the presence of zinc, a zinc ion was observed in an identical position in the active site (data not shown), which again may support the contention that the RPE reaction mechanism could involve the use of a catalytic metal ion to stabilize a 2,3-enediolate intermediate. Interestingly, the active site of RPE bears some likeness to the active site of a distantly related enzyme, 3-keto-L-gulonate 6-phosphate decarboxylase (KGPDC), which is metal-ion-dependent (Wise & Rayment, 2004). Although the side chains of catalytic residues in the active are not conserved, an aspartate and a glutamate in the active site that are homologous to His36 and His68 in the RPE active site serve as ligands for a magnesium ion, further hinting that a metal ion might bind in the RPE active site.

Three highly conserved methionine residues, Met40, Met70 and Met141, are also found in almost identical positions in each of the RPE active sites. The functions of these three residues are also uncertain, although their highly conserved positions in the active site suggest some role in the reaction mechanism. One suggestion is that the S atoms on these three methionines act as a 'polar cushion' to help stabilize a 2,3-enediolate reaction intermediate (Kopp *et al.*, 1999). It is more likely that the hydrophobic environment created by these three

residues serves to alter the electrostatic environment in the active site to acidify the C3 proton of the substrate or perhaps make Asp37 and Asp179 more basic. While the identities of these three residues are methionines in virtually all known RPE homologs, in a few examples other hydrophobic residues are substituted for methionine at these positions, which could presumably carry out a similar function.

A complete understanding of the catalytic mechanism of the RPE reaction will require further structural and biochemical studies. The similarities in the structure of the active site of seRPE described here to those of the two other RPEs for which structural information is known further support essential catalytic roles for strictly conserved residues in the active site.

This research was supported by Grants GM-52594 (to JAG and IR) and GM-65155 (to JAG and IR) from the National Institutes of Health. ELW was supported by NIH Biophysics Training Grant GM08293. Use of the Argonne National Laboratory Structural Biology Center beamline at the Advanced Photon Source was supported by the US Department of Energy, Office of Energy Research under Contract No. W-31-109-ENG-38.

References

Chen, Y. R., Larimer, F. W., Serpersu, E. H. & Hartman, F. C. (1999). *J. Biol. Chem.* **274**, 2132–2136.

Cohen, G. H. (1997). *J. Appl. Cryst.* **30**, 1160–1161.

Collaborative Computational Project, Number 4 (1994). *Acta Cryst.* D**50**, 760–763.

DeLano, W. L. (2002). *The PyMol Molecular Graphics System.* San Carlos, CA, USA: DeLano Scientific.

Eicks, M., Maurino, V., Knappe, S., Flugge, U. I. & Fischer, K. (2002). *Plant Physiol.* **128**, 512–522.

Jelakovic, S., Kopriva, S., Suss, K. H. & Schulz, G. E. (2003). *J. Mol. Biol.* **326**, 127–135.

Jogl, G., Tao, X., Xu, Y. & Tong, L. (2001). *Acta Cryst.* D**57**, 1127–1134.

Karmali, A., Drake, A. F. & Spencer, N. (1983). *Biochem. J.* **211**, 617–623.

Kopp, J., Kopriva, S., Suss, K. H. & Schulz, G. E. (1999). *J. Mol. Biol.* **287**, 761–771.

Kopriva, S., Koprivova, A. & Suss, K. H. (2000). *J. Biol. Chem.* **275**, 1294–1299.

Laskowski, R. A., MacArthur, M. W., Moss, D. S. & Thornton, J. M. (1993). *J. Appl. Cryst.* **26**, 283–291.

Murshudov, G. N., Vagin, A. A. and Dodson, E. J. (1997). *Acta Cryst.* D**53**, 240–255.

Otwinowski, Z. & Minor, W. (1997). *Methods Enzymol.* **276**, 307–326.

Rayment, I. (2002). *Structure*, **10**, 147–151.

Roussel, A. & Cambillau, C. (1991). *Silicon Graphics Geometry Partners Directory.* Mountain View, CA, USA: Silicon Graphics.

Terwilliger, T. C. & Berendzen, J. (1999). *Acta Cryst.* D**55**, 849–861.

Wise, E. L. & Rayment, I. (2004). *Acc. Chem. Res.* **37**, 149–158.